Original Research Article
Determination of Optical Band Gap energy of wurtzite ZnO:Ce Nanocrystallites

ABSTRACT

Aim: Determination of optical band gap energy of ZnO:Ce nanocrystallite and effect of doping on the optical band gap energy also probed.

Material and Methods: ZnO nanoparticles are prepared by chemical precipitation route using 1 molar solution of Zinc acetate solution and Sodium hydroxide solution at 60°C. The I molar percentage (1.72 gm) of Cerium oxide solution is also mixed with the above solutions using magnetic stirrer. Four-five drops Tri Ethyle Amine was are added as capping agent to prevent agglomeration. The characterization of sample was studied by XRD, FESEM, FTIR. TEM. The UV-Vis spectrometer was used to study the Optical properties of nanopowder

Results and discussions From the XRD techniques the crystallite size of ZnO nanopowder was determined as13.83 nm at 150˚C which increased to 16.13 nm at temperatures 180˚C. FESEM showed nanoparticle of average size 13-50nm and nano clusters have size of 1μm. EDAX data is found as Zinc oxide with 99.4% and Cerium 0.6%.TEM confirm the formation ZnO:Ce nanoparticle and it has an average size about 25nm, Some nanorods with average diameter of 40 nm and length of about 290 nm were also observed. The UV absorption spectra for bulk ZnO,nanoparticles of ZnO displayed excitonic peaks at 375 nm and 369 nm respectively. The present study found absorption edge at 372 nm for ZnO:Ce nanoparticle.

Coclusion: The UV Absorption spectra showed red shift towards 372 nm due to doping with Cerium and blue shifted relative to Bulk ZnO. From the absorption spectra optical band gap is determined as 3.32 eV. It was found that energy band gap E_g decreases with doping of Ce. The analysis of optical properties shows that ZnO:Ce is promising dielectric material and has potential application in optoelectronic devices

Keywords: Nanomaterials, Doping, Optical properties

1 INTRODUCTION

Zinc Oxide , a typical II-VI compound semiconductor , with direct band gap of 3.2 eV at room temperature and 60meV as excitonic binding energy , is a very good luminescent material used in displays, UV-Vis laser, solar cell components, gas sensors and varistors [1].Zinc oxide doped with Ce is a transparent electro conductive and piezoelectric material. Zinc Oxide is an excellent Ultraviolet absorber and antibacterial agent. ZnO has been used in solar cells, transparent electrodes, and blue UV light emitting devices. This nanomaterials is a promising candidates for nano-electronic and photonics [1, 2]. It may also be possible to observe coherent emission without population inversion induced by Bose- Einstein condensation at the lower polariton band [3]. ZnO is more resistant to radiation and is multifunctional with uses in the areas as piezoelectric, ferroelectric and ferromagnetic [4]. ZnO: Ce is hexagonal in symmetry with Space group P6$_{3mc}$ and Lattice parameters [2] a = 3.253 Å, b = 3.253 Å, c = 5.209 Å . The stable structure of ZnO is wurtzite [1]. A substantial effort is therefore placed on utilizing such properties within a new generation of short wavelength photonic devices [4]˙In order to get better photo catalytic activity, the incorporation of rare earth ion doping could increase the photo current response and the separation of

45 electron hole pairs under UV illumination [5].Since CeO2 has a band gap of ~3eV and shows the
46 fascinating properties that are similar to that of ZnO, the mixed of both materials have been investigated
47 for the probing of highly efficient Photo catalysis [6].·The dopant sites defects induced by the doping have
48 strong impact on the structural and optical properties of Ce doped ZnO [7]. In this paper we report optical
49 study and on the effect of Ce ion as a dopant in ZnO nanoparticle.

50 **2. MATERIAL AND METHODS**

51
52 **2.1Synthesis and Characterization**

53 ZnO nanoparticles are prepared by chemical precipitation route using 1 molar solution of Zinc acetate
54 solution and Sodium hydroxide solution at $60^{o}C$. The I molar percentage (1.72 gm) of Cerium oxide
55 solution is also mixed with the above solutions using magnetic stirrer. The precipitate obtained is washed
56 with double distilled water many times and acetone and filtered well. Four-five drops Tri Ethyle Amine
57 (TEA) was are added as capping agent to prevent agglomeration. After centrifugation the precipitate is
58 placed in the furnace at 150 and 180˚C. The samples are powdered well in the crucible. The orientation
59 and crystallinity of the powder were studied using Rigaku DMAX diffractometer using Cu -Kα radiation
60 monochromatised with a graphite crystal and high temperature attachment in θ-2θ geometry. The surface
61 topography and microstructure were studied using Field Emission Scanning Electron Microscopy
62 (FESEM) with a Hitachi Model s-3000H Electron microscope. Fourier Transform Infrared spectroscopy
63 (FTIR) uses Nicolet (Impact 410) FTIR Michelson interferometer to produce an interferogram. Energy
64 Dispersive X-ray Spectrum Analysis (EDX) was used to determine percentage composition of Ce in
65 ZnO.The Transmission electron microscopy (TEM) was performed by JEOL 1010,TEM operating at an
66 accelerating voltage of 100keV. Perker Elmer Lamda 25 UV-Vis spectrometer was used to study the
67 Optical properties of nanopowder.

68 **3. RESULTS AND DISCUSSIONS**

69 **3.1 Determination of particle Size from XRD Pattern.**

70 The XRD pattern, Fig. 1, consists of sharp intense peaks of ZnO:Ce which confirms the good crystalline
71 nature of ZnO and peaks originated from (100), (002), (101), (102), (110), (103), (112), (201), (200) and
72 (202) reflections of hexagonal ZnO [4,5]. The XRD techniques are widely used for the particle size
73 determination and structure determination of nanoparticles. The patterns are compared with JCPDS file
74 No:80-0075 comparing the observed data with the JCPDS file. In XRD no peaks are identified to represent
75 Ce due to the small percentage of Ce incorporated into the lattice matrix of ZnS. Due to doping there will
76 not be any change in the structure of ZnS. Only a lattice strain can be observed.
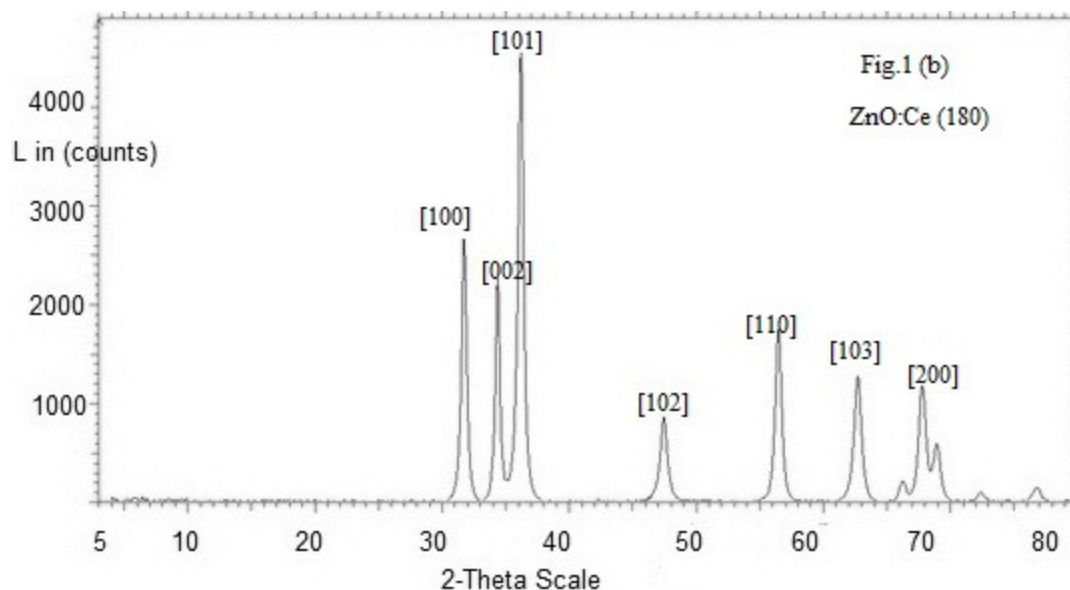
77

Fig 1(a)

ZnO:Ce (150)

78
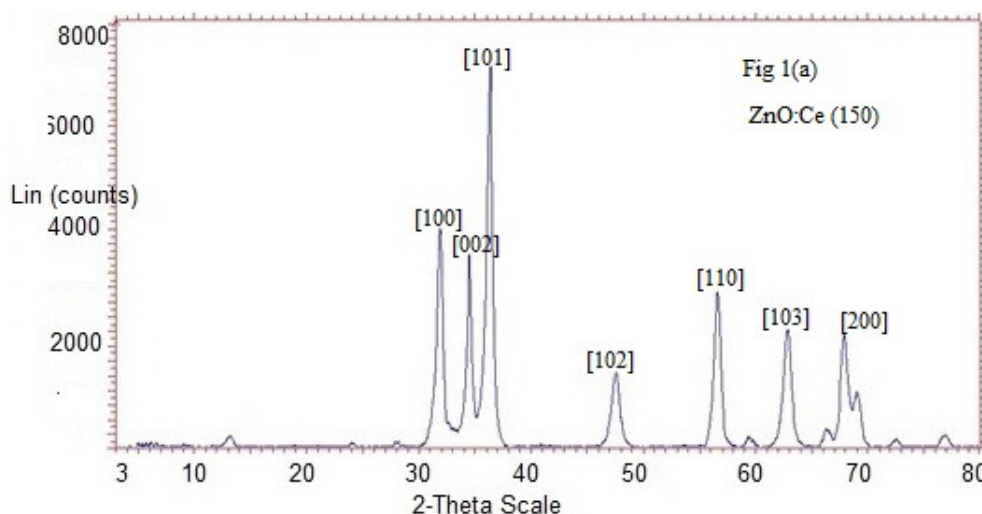
Fig.1(a-b) XRD patterns of ZnO: Ce nanoparticles at 150 and 180°C.

The degree of crystallinity of nanoparticles increases with annealing temperature. The percentage of lattice contraction with annealing temperature can also be studied using X-ray diffraction pattern. Particle Size, can be calculated by the formula [4,7], Debye- Scherrer's formula

$$D = K\lambda / \beta Cos\theta \qquad (1)$$

K= 0.89, λ the X-ray wavelength = 0.154095 nm, β the full width at half maximum and θ the half diffraction angle. The crystal sizes of ZnO:Ce nano particles synthesized at 150 and 180°C were calculated from FWHM and tabulated in Table 1

Table 1.Variation of Grain size of ZnO:Ce with temperature

Temperature °C	FWHM	$\beta \times 10^3$	2θ	θ	Particle size(D) nm
150	0.653	11.39	56.64	28.32	13.83
180	0.560	9.768	56.515	28.257	16.13

From the Fig.1(a-b) it was found that the crystallite size of ZnO nanopowder was 13.83 nm at 150˚C which increased to 16.13 nm at temperatures 180˚C. From the above study, it is observed that there is a continuous increase in the particle size with temperature. The increase in the particle size is due to the amalgamation of the smaller particles into larger particels [8] is a result of solid state diffusion.

3.2 Fourier Transform Infrared Spectrum Analysis.

FTIR spectrum,Fig. 2, has been shown that as particle size decreases, increase in frequency for the bond (blue shift) is observed in nanoparticles. Bands at 416.35 cm^{-1} is assigned to the stretching vibrations of Zn-O. The stretching frequency of bulk ZnO is 424 cm^{-1}. Here a blue shift is observed in that frequency i.e., that frequency due to quantum confinement. Three intense bands were centered at 1384.34 cm^{-1}, 1041.54 cm^{-1} and 1556.58 cm^{-1} and are attributed to the stretching vibrations of C = O, C = C and C-H groups in acetate species, which suggests its presents as absorbed species in the surface of

101   nanoparticles. The broad absorption peak centered at 3423.61 cm^{-1} and 1626.40 cm^{-1} corresponds to O-
102   H stretching and bending frequencies of H_2O, indicating the existence of water in the surface of
103   nanoparticles [9]. The peak observed at 825.80 cm^{-1} may be the presence of some impurities in the Zinc
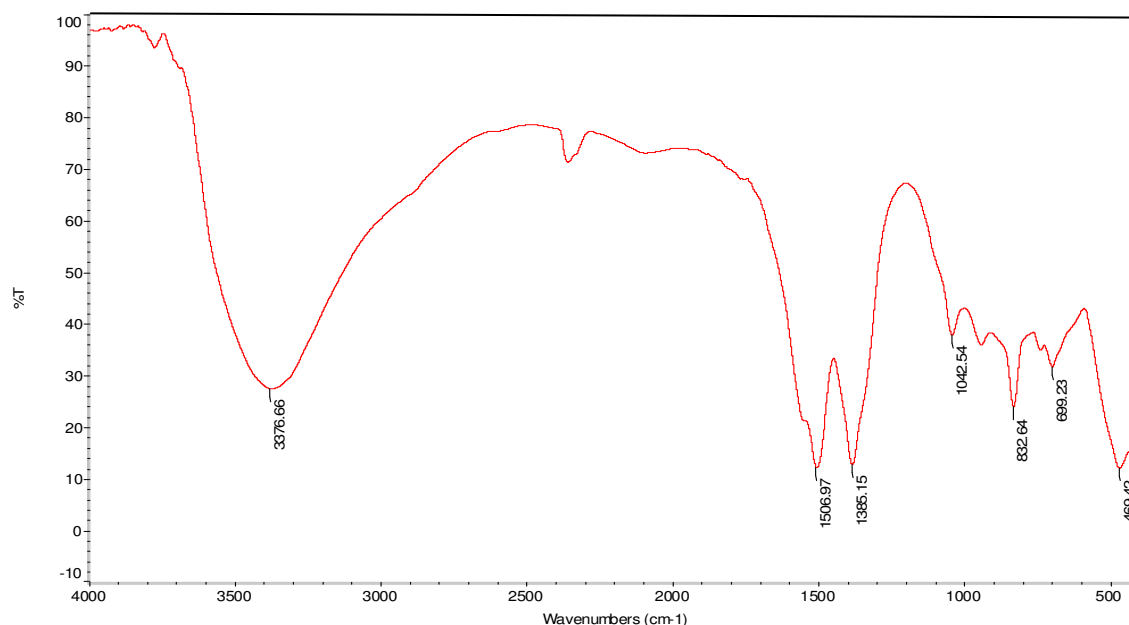104   Acetate or Zinc Oxide nanoparticle

105

106   **Fig.2. Fourier Transform Infrared Spectrum of ZnO:Ce nanorods**

107   **3.3 Scanning Electron Microscopy (SEM).**

108   The Scanning electron micrographs of ZnO:Ce nanomaterials synthesized under aqueous medium. The
109   orientation growth of ZnO crystal in water is higher [6].spear shaped morphology is observed in the
110   micrograph of ZnO:Ce. The SEM pictures, Fig.3, showed distinguished rod like l morphology with self
111   aligned prismatic nanoparticles. The morphology of ZnO:Ce nanopowder as revealed by FESEM showed
112   nanoparticle of average size 13-50 nm In SEM measurement the grain size is measured and calculated
113   by taking the noticeable grain boundaries. While in the case of XRD measurements are taken from the
114   crystalline area that diffracts the X-ray waves. Thus the XRD measurement size of capped ZnS particle
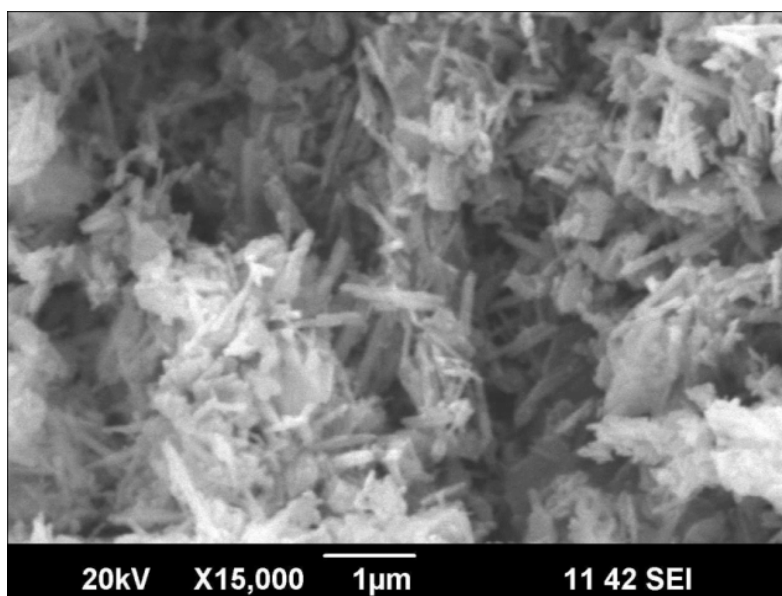115   was found to be smaller that the size found when using SEM measurement [10].

116

Fig.3 SEM image of ZnO:Ce Nanorods under high magnification

3.4 Energy Dispersive Spectrum Analysis (EDS).

This technique is used for identifying the elemental composition of the specimen. The higher a peak in a spectrum, the more concentrated the element is in the spectrum.
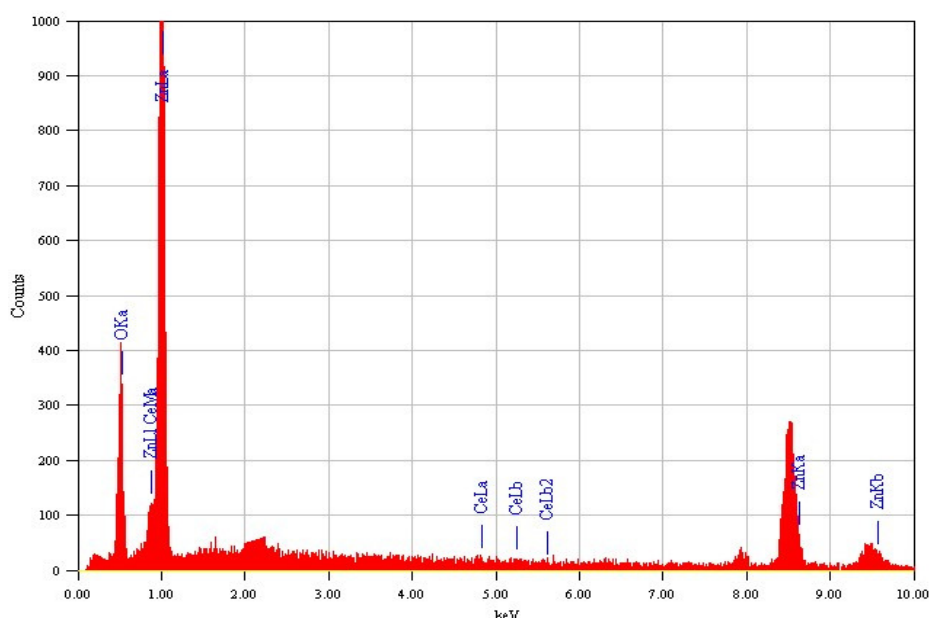

121

Fig 4 EDAX of ZnO:Ce nanorods

An EDS spectrum plot not only identifies the element corresponding to each of its peaks, but the type of X-ray to which it corresponds as well. For example, a peak corresponding to the amount of energy possessed by X-rays emitted by an electron in the L-shell going down to the K-shell is identified as a K-Alpha peak. The peak corresponding to X-rays emitted by M-shell electrons going to the K-shell is identified as a K-Beta peak. High intensity peaks for Zn, O_2 and Ce. EDS ,Fig.4 of ZnO:Ce nanoparticle is plotted using the recorder and the EDAX data is found as Zinc oxide with 99.4% and Cerium 0.6%. *i,e,*

129 very small percentage was incorporated in to the ZnO matrix due to incompatible size of the impurity
130 atom.

3.5 Transmission Electron Microscopy (TEM)

132 Fig.5(a,b) show typical TEM Images, after 4 hours photo development , of a single ZnO:Ce nanorods to
133 confirm the crystal quality and growth direction. It is clear from TEM image that the end of the ZnO:Ce
134 nanorod is sharp tip. TEM confirm the formation ZnO:Ce nanoparticle and it has an average size about
135 25nm, Some nanorods with average diameter of 40 nm and length of about 290 nm were also
136 observed.TEM showed that the particles have nanometric prism like and rod like morphologies. The cross
137 section of the one dimensional (1D) nanostructure include triangle, hexagonal and rectangle shapes. High
138 Resolution Transmission Electron Microscopic (HRTEM) pattern indicates that the nanorods grow along
139 the c-axis and it has standard hexagonal structure.
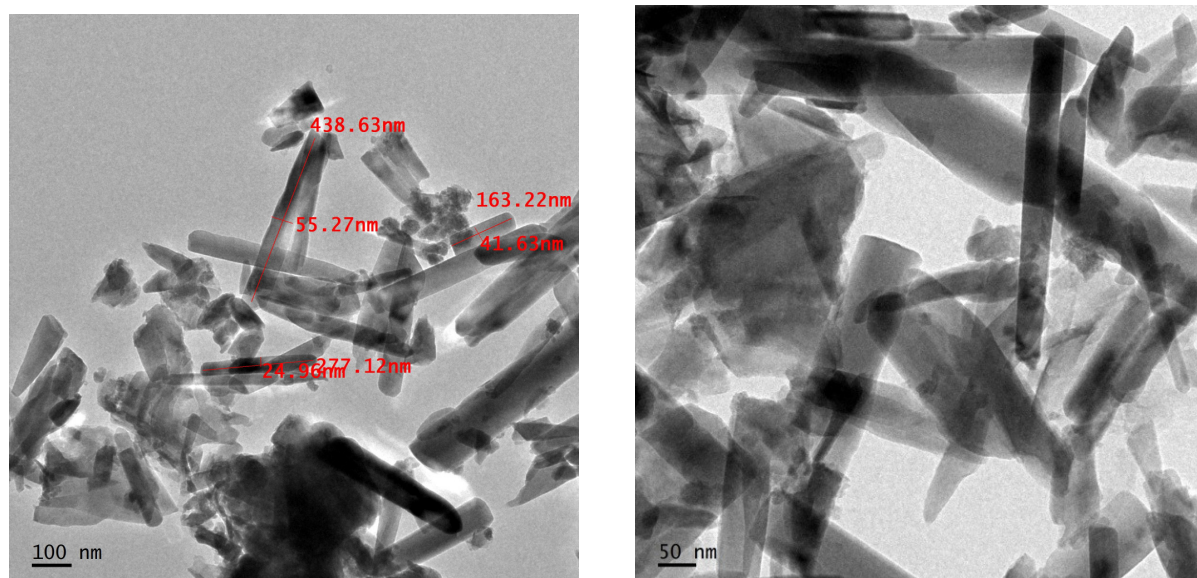
140

141 **Fig.5 (a-b) TEM images of ZnO:Ce nanorods**

3.6 UV Absorption Spectra

3.6.1 Optical Band gap energy from UV absorption Spectra.

144 Energy band gap studies of these materials have been reported using absorption spectra. The Fig.6(a-b)
145 depict the optical absorption spectrum of undoped ZnO nanoparticle and ZnO:Ce nanopowder prepared
146 under aqueous conditions. A size-dependent electron-hole exchange interaction is also responsible for it
147 and has been reported [12, 14]. The optical band gap energy can be computed using the relation where
148 $h,$ the Planck's constant, c velocity of light and λ_g wavelength corresponding to the absorption maximum.
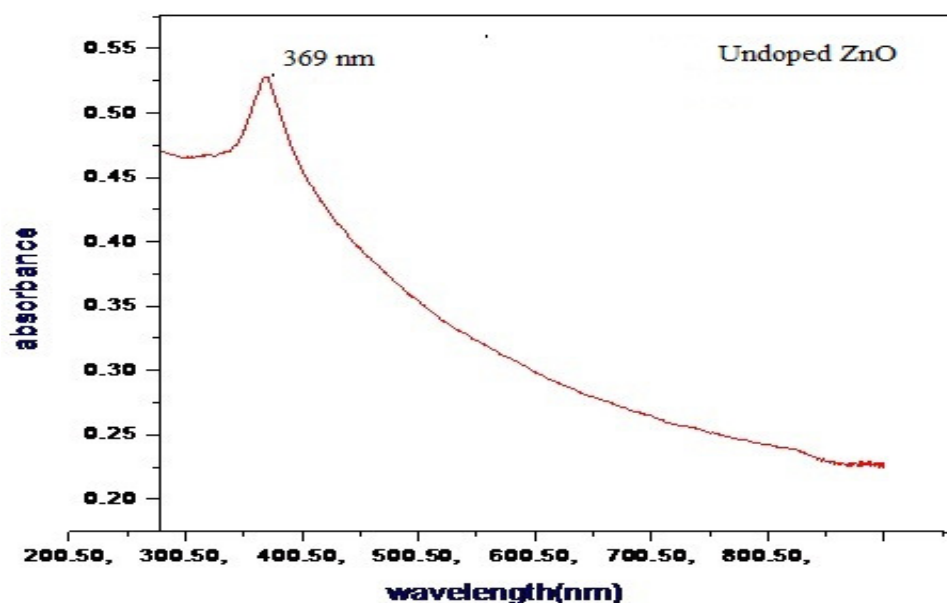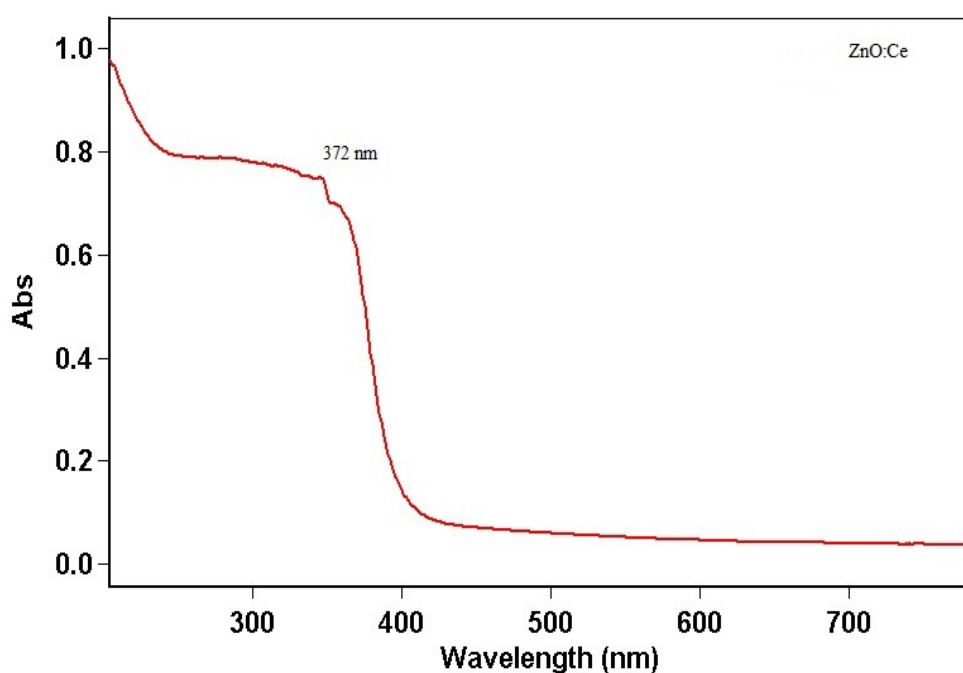
Fig.6(a) UV spectrum of ZnO

Fig 6(b) UV Spectrum of ZnO:Ce nanorods

$$E_g = h\nu_g = hc / \lambda_g \qquad (2)$$

The UV absorption spectra for bulk ZnO, nanocrystallite of ZnO displayed excitonic peaks at 375 nm and 369 nm respectively [7, 13]. The present study revealed that The UV visible spectra absorption edge is at 372 nm (3.32 eV) for nanocrystallite of Zinc Oxide doped with rare earth ion Cerium. The values are tabulated in the Table 2. It has displayed a red shift 5 nm for absorbance. It is found that after the Ce

159 incorporation, a new localized band appears between the valence and conduction band, which
160 corresponds to the majority spin of Ce - 4f states [16]. It is this localized band constructs a bridge
161 between the valence and conduction state, which will improve the optical performance of ZnO. ZnO:Ce is
162 a degenerate semiconductor. The strong correlation effect is very important for the 4f of the Ce atom in
163 ZnO:Ce. The mismatch of the majority and minority spin of Ce-4f, Ce-5d state and the spin polarized
164 holes in O-2p state induced by Ce doping leads to the presence of magnetic order for ZnO:Ce. The
165 analysis of optical properties shows that ZnO:Ce is promising dielectric material and has potential
166 application in optoelectronic devices [15]. The introduced dopant ions might shape a shallow energy level
167 near valence band. Hence we assign the red shift to the defects and the probable shallower energy levels
168 [17]. Therefore, the optical band gap of Ce doped ZnO is broader than that of undoped Zinc Oxide. Hence
169 the value of band gap energy lies in the higher wavelength region. The changes in band gap were due to
170 the existence of a valence band-donor transition at 3.38 eV which can dominate the absorption spectrum
171 when the bulk, as distinct from the surface, of a single crystal is probed.

172 **Table 2:Band gap energy of Bulk ZnO, nanoparticle of ZnO and ZnO:Ce nanoparticle**

Sample material	Band Gap energy E_g (eV)	Wavelength Maximum λ_{gn}(nm)
ZnO: Ce Nanomaterials	3.32	372
ZnO Nanomaterials	3.38	369
ZnO Bulkmaterial	3.3	375

173

174 4. CONCLUSIONS

175

176 The size and crystal structure of ZnO doped with Cerium was studied using XRD. The XRD results
177 indicated that the particle size of nano ZnO:Ce is much small as compared to that of pure ZnO and
178 decreases with the cerium loading. From the XRD results, it is clear that as temperature increases,
179 particle size also increases. The change in particle size cause large variation in the physical properties.
180 High temperature XRD also confirmed that the nanoparticles were stable not only at room temperature
181 but at high temperature as well. The UV Absorption spectra showed red shift towards 372 nm due to
182 doping with Cerium. From the absorption spectra obtained by UV-Vis spectrometer the   optical band gap
183 is determined and found to be in the range 3.32 eV. It was found that energy band gap E_g decreases with
184 doping of Ce. Doping of Ce changed the free carrier concentration in the ZnO nanoparticles [15]. The
185 analysis of optical properties shows that ZnO:Ce is promising dielectric material and has potential
186 application in optoelectronic devices .

187

188 REFERENCES

189 1   Karpina VA., Crys.Res.Tech, 2004; 39; 980.

190 2   Bernal R, Cruz VC, Optical Materials, 2005; 27 12; 35.

191 3   Imamoglu R J, Yamamoto Y, Phys.Rev A ,1996; 53; 4250.

192 4   Kumbhakar P, Singh D, Chalcogenide Letters, 2008; 5; 387.

193 5   Liu TX,Li XZ, Li FB, Chemical Engineering Journal, 2010; 157(2-3);475

194 6   Li GR, Lu XH, Lu XW, Zhao X, Tang YX, Crystal growth Design, 2008; 8(2);1276.

195   7   Yang JH, Gao M,Wang YX, Fan HG, Applied Surface Science, 2008; 255 (5); 2646.

196   8   Nanda K K, Kruis F E, Hassan H, Phys.Rev.Lett. 2002; 89; 256103.

197   9   Xu, Love, L C, Wolfe D B, Whitesides G M, Annu.Rev.Mater.Res. 2004;34**;**339.

198   10   Shashi B Rana,Amarpal singh, Electronic Material Letters,2014,13,212
199
200   11   Srikant V, Clarke D R, J.Appl.Phys, 1998; 83; 5447.

201   12   Chang HJ,Cheng ZL ,J of Korean Physical Society**,** 2004; 45(4);959.

202   13   Soosan S, Lekshmi B, SB Academic Review,2009; 1-2; 57.

203   14   Tingting Ren, Holly RB, Thin Solid Films, 2007; 515**;** 7976.

204   15   Iqbal J, Liu XF, Zhu XC ,Yu RH, J.Applied Phys. 2009; 106; 835115.

205   16   Ali Fathima A, Suganthi Devadason, J Pure Applied & Industrial Physics, 2011; 1 (2); 115-120.

206   17   Nadia Febiana, Djaja,Roseri, Saleh, Mat. Sci & Applications, 2013; 4; 145-152.

207

208

209